Correlation between Magnetic Properties and Mn/Co Atomic Order in $LaMn_{0.5}Co_{0.5}O_{3+\delta}$. 2. Magnetic and Calorimetric Properties

Tôru Kyômen, Ryutaro Yamazaki, and Mitsuru Itoh*

Materials and Structures Laboratory, Tokyo Institute of Technology, 4259 Nagatsuta, Midori-ku, Yokohama 226-8503, Japan

Received May 27, 2003. Revised Manuscript Received October 30, 2003

Correlation between magnetic properties and Mn/Co atomic order in $LaMn_{0.5}Co_{0.5}O_{3+\delta}$ was investigated by powder X-ray diffraction, dc magnetization, ac magnetic susceptibility, and heat capacity measurements. The Mn/Co atomic order was controlled by annealing at some temperatures and successive quenching. The qualitative and quantitative magnetic properties depend on whether the annealing temperature is above or below 1400 K. The samples annealed below 1400 K showed a clear heat capacity anomaly and deviation from Curie−Weiss law due to ferromagnetic critical fluctuation. On the other hand, the samples quenched from above 1400 K showed an unclear heat capacity anomaly, downward deviation from Curie−Weiss law, and asymmetric $M-H$ loop after high-field cooling. These results suggest that the long-range ordering of the Mn/Co atomic configuration occurs at around 1400 K, that the long-range ferromagnetic ordering occurs only when the long-range order of Mn/Co atomic configuration is present, and that ferromagnetic clusters form in a paramagnetic matrix when the long-range order of Mn/Co atomic configuration is absent. The frequency dependence of ac magnetic susceptibility, retardation to ac field, and coercive force showed a maximum when the sample was annealed at around 1400 K, which were discussed in relation to the fluctuation of Mn/Co atomic order.

Introduction

The purpose of the present study is to clarify a relation between atomic order and magnetic properties in a solid−solution system. It is supposed that magnetic properties are affected by three parameters characterizing atomic order.[1] Figure 1 shows the general temperature dependence of three parameters when a long-range ordering of atomic configuration occurs through an order−disorder phase transition of second-order type at T_C^a. Two of them are average long-range and short-range order parameters and the other is fluctuation of order parameter. The order parameters should fluctuate thermally at high temperature and thus "average" means time average and the fluctuation is the standard deviation. The average long-range order parameter is zero above T_C^a and finite below T_C^a. The average short-range order parameter is finite above and below T_C^a. Both order parameters increase monotonically with decreasing temperature. On the other hand, the order fluctuation diverges at T_C^a due to the critical fluctuation and decreases above and below T_C^a.

In the previous paper (part 1),[2] relaxation times of Mn/Co atomic ordering in a rock-salt type in $LaMn_{0.5}Co_{0.5}O_{3+\delta}$ were investigated in relation to the structural change. $LaMn_{0.5}Co_{0.5}O_{3+\delta}$ was found to be an appropriate material for the present purpose since the above three parameters characterizing the Mn/Co atomic order can be controlled easily by thermal treatment because of the moderate relaxation time (about 10 h) at around T_C^a. Here, the valence state of Mn/Co ions is important for the present study because of the following reasons: (1) The ground valence state of Mn/Co ions is Mn^{4+}/Co^{2+}(high spin) in the completely long-range ordered phase with respect to the Mn/Co atomic configuration (long-range and short-range order parameters are 1).[2−7,9] (2) The Mn^{3+}/Co^{3+}(high spin) state is mixed by disordering the Mn/Co atomic configuration, even at zero Kelvin, or by increasing the temperature, even in the completely long-range ordered phase due to thermal excitation.[2] (3)

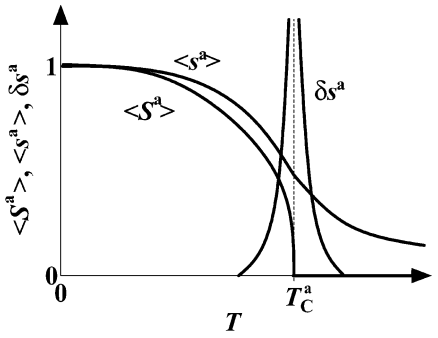

Figure 1. Temperature dependence of average long-range order parameter ($\langle S^a\rangle$), average short-range order parameter ($\langle s^a\rangle$), and fluctuation of order parameter (δs^a) with respect to an atomic configuration when the long-range atomic ordering takes place through an order−disorder phase transition of second-order type at T_C^a.

* To whom correspondence should be addressed.

(1) Stanley, H. E. *Introduction to phase transitions and critical phenomena*; Clarendon Press: Oxford, 1971.

(2) Kyômen, T.; Yamazaki, R.; Itoh, M. *Chem. Mater.*, in press.

10.1021/cm030279t CCC: $27.50
Published on Web 12/05/2003

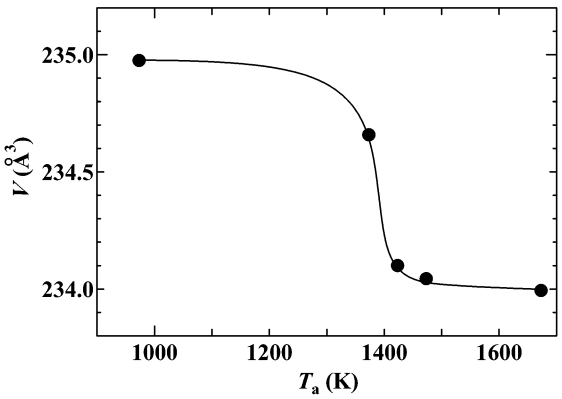

Figure 2. Annealing temperature dependence of unit cell volume at room temperature. Solid circles are experimental value. The solid line is a guide for the eye.

Therefore, the unit cell volume at room temperature is a qualitative indicator for the order parameter of Mn/Co atomic configuration because the average ion radius of Mn^{4+}/Co^{2+} is larger than that of Mn^{3+}/Co^{3+} and the thermal excitation of the valence state is small around room temperature.

In the present paper (part 2), magnetic and calorimetric properties of $LaMn_{0.5}Co_{0.5}O_{3+\delta}$ below room temperature are reported for some samples whose Mn/Co atomic order is controlled by quenching the sample followed by annealing for a long time, time enough to equilibrate the Mn/Co atomic configuration. It is found that magnetic properties are classified into three groups correlated with the long-range order parameter, short-range order parameter, and order fluctuation of Mn/Co atomic configuration.

Experimental Section

A $LaMn_{0.5}Co_{0.5}O_{3+\delta}$ polycrystalline sample was prepared by a solid-state reaction method reported previously.[2] In addition to the quenched (quenched from 1673 to 300 K) and slowly cooled (cooled at 10 K/h from 1673 to 973 K) samples used for the previous study,[2] some samples were prepared as follows. The slowly cooled sample was annealed at a temperature for 40−100 h, and then the sample was quenched in air at room temperature. The annealing temperature is defined as T_a and the sample is referred to as T_a annealed sample in this paper. The annealing time is at least 4 times larger than the relaxation time at each T_a estimated from eq 1 in the previous paper.[2] The excess oxygen composition, $\delta \approx 0.04$, does not change at least below 1573 K, which has already been reported in the previous paper.[2] Lattice parameters at room temperature were determined from powder X-ray diffraction peaks using Si as an internal standard (Cu Kα; MAC Science, MXP18HF). dc magnetizations were measured using a SQUID magnetometer (Quantum Design, MPMS5S). ac magnetic susceptibilities were measured in the range 5−300 K with an amplitude of 10 Oe and frequencies of 10 Hz, 100 Hz, 1 kHz, and 10 kHz using a Physical Property Measurement System (Quantum Design, PPMS). Heat capacities were measured by a relaxation method in the range 2−300 K and under 0 and 90 kOe using PPMS.

Results

Unit Cell Volume at Room Temperature. Figure 2 shows the annealing temperature dependence of unit cell volume at room temperature. All samples have an orthorhombic unit cell. The unit cell volume at room temperature looks like it is decreasing abruptly when

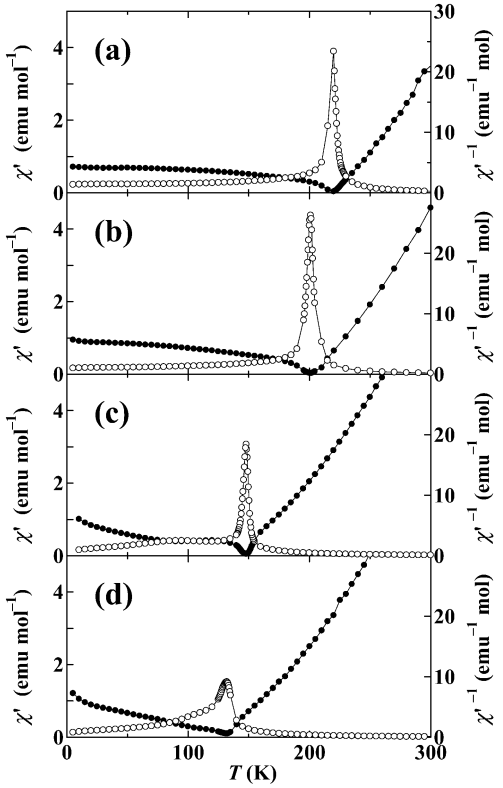

Figure 3. Real part (open circles) and reciprocal real part (solid circles) of ac magnetic susceptibility at 10 Hz: (a) slowly cooled sample; (b) 1373 K annealed sample; (c) 1423 K annealed sample; (d) quenched sample.

T_a is increased above 1400 K. T_a of slowly cooled and quenched samples were plotted tentatively as 973 and 1673 K, respectively. However, the Mn/Co atomic configurations of slowly cooled and quenched samples at room temperature might be different from each equilibrium, one at the T_a because the relaxation time of Mn/Co atomic ordering is large (∼800 h) at 973 K and small (∼1 h) at 1673 K according to eq 1 in the previous paper.[2] On the other hand, the Mn/Co atomic configuration of the other samples at room temperature must be close to the equilibrium one at each T_a because the relaxation times, 5−20 h, are short as compared to the annealing times, 40−100 h, and too long for the Mn/Co atomic configuration to change during the quenching process. Therefore, the abrupt decrease in the unit cell volume at room temperature when T_a is increased above 1400 K implies that the equilibrium Mn/Co atomic configuration abruptly changes around 1400 K. Taking into account the fact that the long-range Mn/Co atomic order has been observed by a neutron diffraction experiment of $LaMn_{0.5}Co_{0.5}O_3$ prepared by slow cooling,[7,8] it is natural to consider that the order−disorder phase transition with respect to the Mn/Co atomic configuration occurs at $T_C^a \approx 1400$ K.

(3) Blasse, G. *J. Phys. Chem. Solids* **1965**, *26*, 1969.
(4) Jonker, G. H. *J. Appl. Phys.* **1966**, *37*, 1424.
(5) Nishimori, N.; Asai, K.; Mizoguchi, M. *J. Phys. Soc. Jpn.* **1995**, *64*, 1326.
(6) Asai K.; Fujiyoshi, K.; Nishimori, N.; Satoh, Y.; Kobayashi, Y.; Mizoguchi, M. *J. Phys. Soc. Jpn.* **1998**, *67*, 4218.
(7) Bull, C. L.; Motimer, R.; Sankar, G.; Gleeson, D.; Catlow, C. R. A.; Wood, I. G.; Price, G. D. *Synth. Met.* **2001**, *121*, 1467.
(8) Bull, C. L.; Gleeson, D.; Knight, K. S. *J. Phys.: Condens. Matter* **2003**, *15*, 4927.

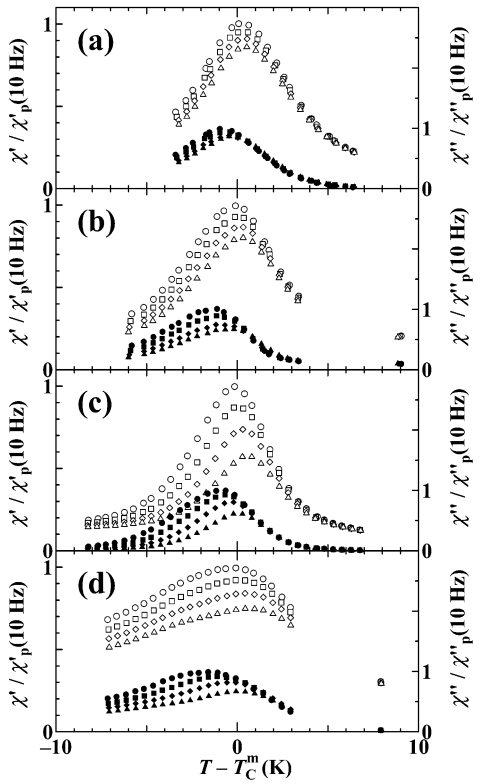

Figure 4. Real (open symbols) and imaginary (solid symbols) parts of ac magnetic susceptibility normalized by each peak intensity at 10 Hz [χ'_p(10 Hz), χ''_p(10 Hz)]. (a) slowly cooled sample; (b) 1373 K annealed sample; (c) 1423 K annealed sample; (d) quenched sample. circles, 10 Hz; squares, 100 Hz; diamonds, 1 kHz; triangles, 10 kHz.

Magnetic Properties. The open circles in Figure 3a−d represent the real parts of ac magnetic susceptibility at 10 Hz for the slowly cooled, 1373 K annealed, 1423 K annealed, and quenched samples, respectively. All samples showed a peak around 220−130 K and the peak temperature decreased with increasing T_a [see Figure 11a]. The peak temperature at 10 Hz is defined as T_C^m in this paper. The solid circles in Figures 3a−d represent the reciprocal real parts of ac susceptibility at 10 Hz. The $\chi'^{-1}-T$ curves of slowly cooled and 1373 K annealed samples showed a downward convex curve down to T_C^m, which is usually observed in a typical ferromagnet due to critical fluctuation. On the other hand, the $\chi'^{-1}-T$ curves of 1423 K and quenched samples showed an upward convex curve just above T_C^m. In addition to the peak at T_C^m, a broad peak or shoulder was observed in the $\chi'-T$ curves of 1423 K annealed and quenched samples around 90 and 100 K, respectively.

Figure 4 shows the frequency dependence of real and imaginary parts of ac susceptibility normalized by each peak intensity at 10 Hz. The peak temperature and intensity depend on frequency in each sample. The difference in the peak temperature of the real part between 10 Hz and 10 kHz is at most 1 K for each sample and it is unclear whether the difference depends on T_a or not. On the other hand, the difference in the peak intensity of the real part between 10 Hz and 10 kHz clearly depends on T_a. Quantitatively, $\{\chi'_p/\chi'_p(10\ \text{Hz})\}^{-1}$ at 10 kHz showed a maximum when $T_a = 1423$ K [see Figure 11e].

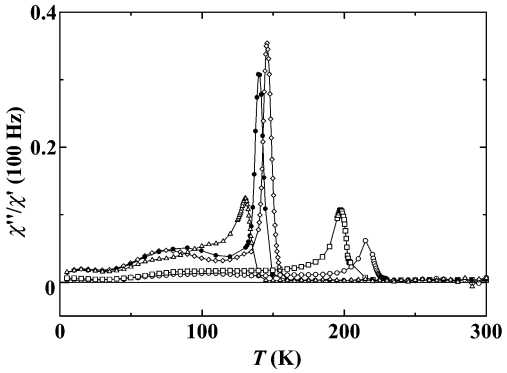

Figure 5. χ''/χ' at 100 Hz: open circles, slowly cooled sample; open squares, 1373 K annealed sample; open diamond, 1423 K annealed sample; solid circles, 1473 K annealed sample; open triangles, quenched sample.

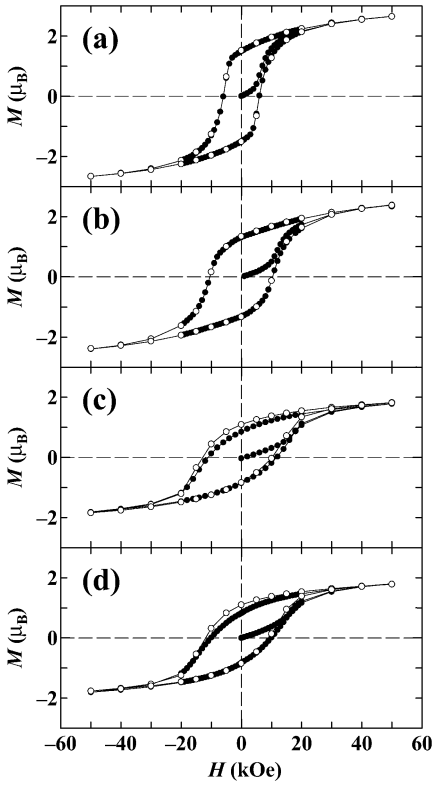

Figure 6. Magnetic field dependence of dc magnetization at 5 K: (a) slowly cooled sample; (b) 1373 K annealed sample; (c) 1423 K annealed sample; (d) quenched sample. Open and solid circles represent the result obtained after zero-field cooling and 50 kOe field cooling, respectively, from 300 to 5 K.

Figure 5 shows the χ''/χ' at 100 Hz that is a tangent of the retardation angle of magnetization to the applied ac field. A peak was observed at around T_C^m in each sample. The peak intensity showed a maximum when $T_a = 1423$ K [see Figure 11d]. The behavior below T_C^m is complex.

Figure 6a−d shows the magnetic field (H) dependence of dc magnetization (M) at 5 K. Two kinds of measurements were carried out. The solid circles represent the result of sequence, 0 → 50 → −50 → 50 kOe, after cooling under zero field from 300 to 5 K. The open circles represent the result of sequence, 50 → −50 → 50 kOe, after cooling from 300 to 5 K under 50 kOe. Both $M-H$ loops coincide with each other within the experimental

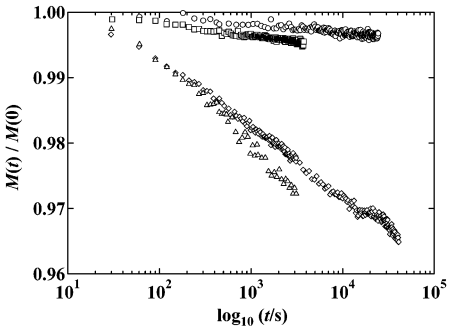

Figure 7. Time dependence of dc magnetization at 5 K and under zero field after 50 kOe magnetic field was turned off: open circles, slowly cooled sample; open squares, 1373 K annealed sample; open diamonds, 1423 K annealed sample; open triangles, quenched sample.

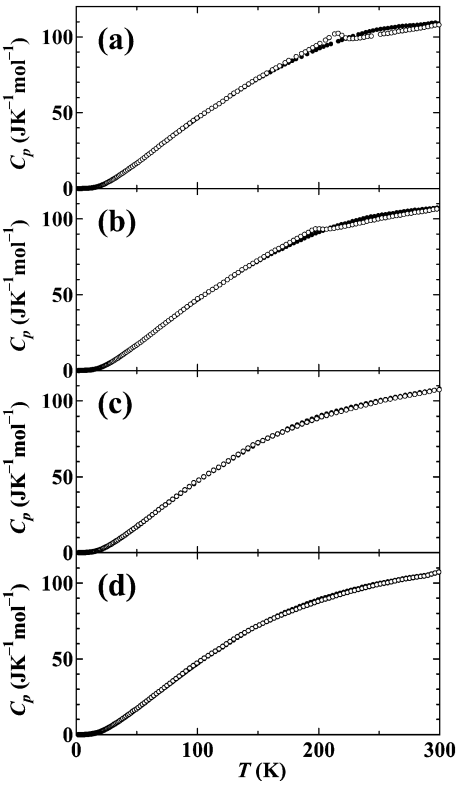

Figure 8. Heat capacities under 0 (open circles) and 90 kOe (solid circles): (a) slowly cooled sample; (b) 1373 K annealed sample; (c) 1423 K annealed sample; (d) quenched sample.

errors for the slowly cooled and 1373 K annealed sample. On the other hand, the center of the $M-H$ loop measured after field cooling shifted to the second quadrant for the 1423 K annealed and quenched samples. The magnetization under 50 kOe decreased with increasing T_a [see Figure 11b]. The coercive force in the $M-H$ loop after zero-field cooling is smallest for the slowly cooled sample and showed a maximum when T_a = 1423 K [see Figure 11c].

Figure 7 shows the time (t) dependence of dc magnetization [$M(t)$] normalized by $M(0)$ at 5 K after the sample was cooled from 300 to 5 K under 50 kOe and the applied field was then turned off, where $t = 0$ is a time when the magnetic field reached at 0 Oe. All samples showed a relaxation phenomenon with nearly linear dependence on log(t/s) similar to Richter-type magnetic aftereffect[10] or thermal fluctuation magnetic aftereffect.[11] This implies a presence of distribution in the relaxation times.

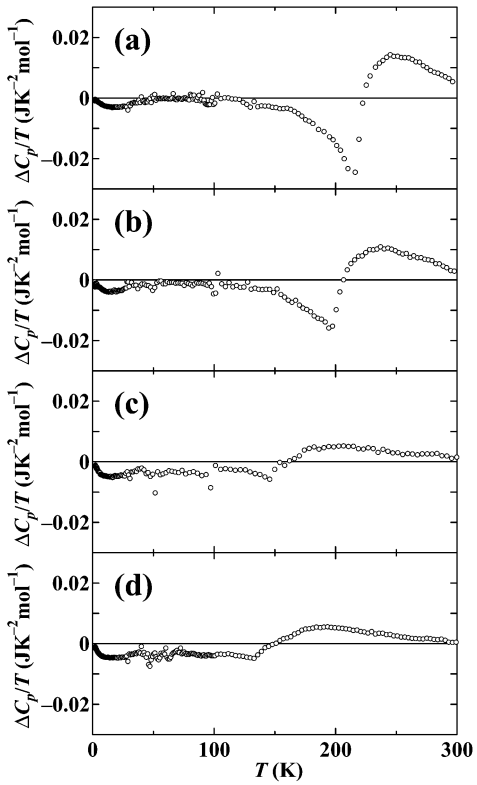

Figure 9. Difference in heat capacity divided by temperature between 0 and 90 kOe; $\Delta C_p = C_p$(90 kOe) − C_p(0 Oe): (a) slowly cooled sample; (b) 1373 K annealed sample; (c) 1423 K annealed sample; (d) quenched sample.

Calorimetric Properties. The open and solid circles in Figure 8a−d represent the heat capacities under 0 and 90 kOe magnetic fields for the slowly cooled, 1373 K annealed, 1423 K annealed, and quenched samples. A clear heat capacity anomaly was observed in the slowly cooled and 1373 K annealed samples around T_C^m. The magnitude and sharpness of anomaly look like they are decreasing in the 1373 K annealed sample as compared to those of the slowly cooled sample. The heat capacity anomaly broadens under 90 kOe because the ferromagnetic fluctuation is suppressed. On the other hand, only a small cusp was detected around T_C^m in the 1423 K annealed and quenched samples.

Figure 9a−d shows the difference in the heat capacity divided by temperature between 0 and 90 kOe. In the slowly cooled and 1373 K annealed samples, the $\Delta C_p/T-T$ curve showed a minimum around T_C^m and changes from negative to positive with increasing temperature just above T_C^m. The qualitatively same characters were also observed in the 1423 K annealed and quenched samples. This concludes that a ferromagnetic-like ordering occurs around T_C^m even in the 1423 K annealed and quenched samples.

Parts (a) and (b) of Figure 10show the heat capacity under zero field and the heat capacity difference between 0 and 90 kOe below 10 K, respectively. The heat capacity and heat capacity difference increased with

(9) Dass, R. I.; Goodenough, J. B. *Phys. Rev. B* **2003**, *67*, 014401.
(10) Richter, G. *Ann. Phys.* **1937**, *29*, 605.
(11) Gaunt, P *Philos. Mag.* **1976**, *34*, 775.

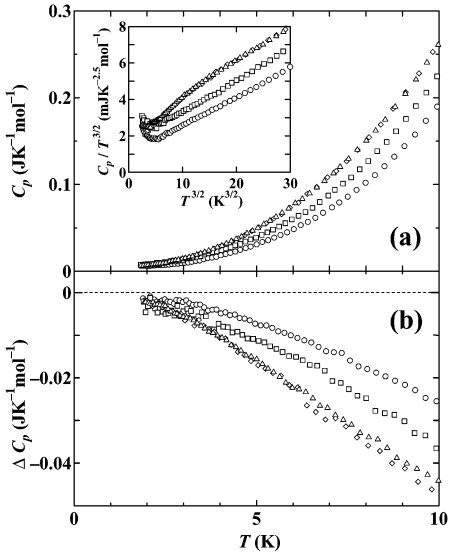

Figure 10. (a) Heat capacities under zero field. Inset shows $C_p/T^{3/2}$ vs $T^{3/2}$ plot. (b) Heat capacity difference between 0 and 90 kOe; $\Delta C_p = C_p$(90 kOe) $- C_p$(0 Oe): open circles, slowly cooled sample; open squares, 1373 K annealed sample; open diamonds, 1423 K annealed sample; open triangles, quenched sample.

increasing T_a but the 1423 K annealed and quenched samples showed a similar magnitude. Because the heat capacity difference originates only from magnetic excitation (not phonon excitation), it is concluded that the increased heat capacity with increasing T_a is mainly due to an increase in magnetic excitation. This is consistent with the result that T_C^m decreases with increasing T_a.

If there is no gap in the spin wave excitation, the heat capacity at low temperature is represented by $C_p = \alpha T^{3/2} + \beta T^3$ and thus $C_p/T^{3/2}$ versus $T^{3/2}$ plot shows a linear curve, where $\alpha = 5.029R(1/8\pi JS)^{3/2}$, R is the gas constant, J is the exchange interaction constant, and S is the spin quantum number.[12] The inset of Figure 10a shows the $C_p/T^{3/2} - T^{3/2}$ plot. The curve of the slowly cooled sample looks like it is linear. However, J estimated from α ($\approx 1.0 \times 10^{-3}$ J K$^{-2.5}$ mol^{-1}) is 32 K ($S = {}^3/_2$) and the paramagnetic Curie temperature estimated from the J by using the mean-field approximation[12] is 480 K for the slowly cooled sample. Because this is much larger than the experimental value, 322 K,[2] it is supposed that there is a gap in the spin wave excitation and that the linear $C_p/T^{3/2} - T^{3/2}$ curve is accidental. This is consistent with the $M - H$ curve, indicating the character of a hard ferromagnet.

Discussion

Figure 11a−e shows the annealing temperature dependence of T_C^m, dc magnetization at 5 K and under 50 kOe, coercive force at 5 K, peak intensity of χ''/χ' at 100 Hz, and reciprocal peak intensity of χ'/χ'_p(10 Hz) at 10 kHz, respectively. Because $(\chi''/\chi')_p$ indicates a degree of magnetization retardation to an applied ac field around T_C^m, this is referred to as a retardation parameter. Because $\{\chi'/\chi'_p(10Hz)\}_p^{-1}$ indicates a degree of frequency dependence of peak intensity around T_C^m, this is referred to as a frequency-dependence parameter.

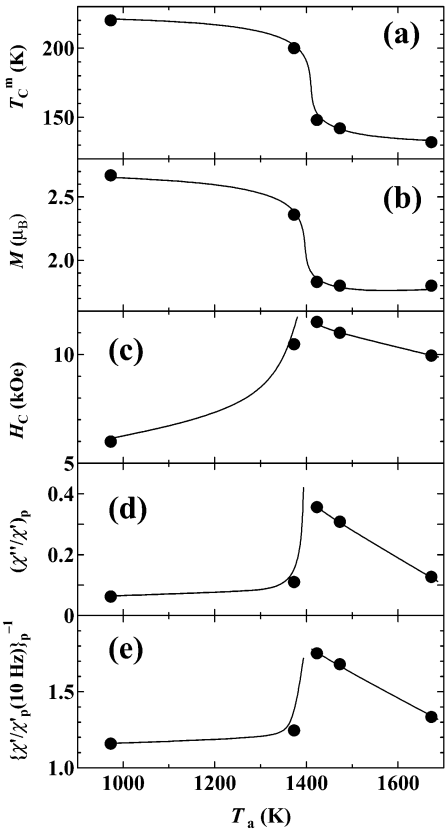

Figure 11. Annealing temperature dependence of (a) T_C^m, (b) dc magnetization at 5 K and under 50 kOe, (c) coercive force at 5 K, (d) retardation parameter, and (e) frequency-dependence parameter. See the text for the definitions of (d) and (e).

It is found that the former two quantities show an abrupt increase or decrease around 1400 K and the latter three quantities show a maximum around 1400 K. This supports the belief that an order−disorder phase transition with respect to the Mn/Co atomic configuration occurs at $T_C^a \approx 1400$ K as mentioned in the Results section. In addition, this indicates that these five quantities are correlated with the Mn/Co atomic configuration. T_C^m and M at 5 K and under 50 kOe show T_a dependence similar to that of the unit cell volume shown in Figure 2. This is plausible because disordering of the Mn/Co atomic configuration should weaken the average ferromagnetic interaction and magnetization due to the appearance of antiferromagnetic pairs such as Co^{2+}−Co^{3+}. This consideration would also explain the result that the heat capacity at low temperatures increases with increasing T_a because magnetic excitation at a certain temperature increases with weakening of the average magnetic interaction. In addition, the disordering should suppress the cooperativity of ferromagnetic ordering and the corresponding critical fluctuation. In fact, the heat capacity anomaly broadens with increasing T_a. The reason for the maximum around 1400 K in coercive force, retardation parameter, and frequency-dependence parameter are discussed below by using Figure 12a−d, which illustrates the Mn/Co atomic configuration in each sample.

The samples annealed below T_C^a showed a downward convex $\chi'^{-1} - T$ curve above T_C^m, a symmetric $M-H$ loop even after high-field cooling, and a clear heat capacity anomaly. These are characteristics of a typical long-

(12) Kittel, C. *Quantum Theory of Solids*; John Wiley & Sons: New York, 1963.

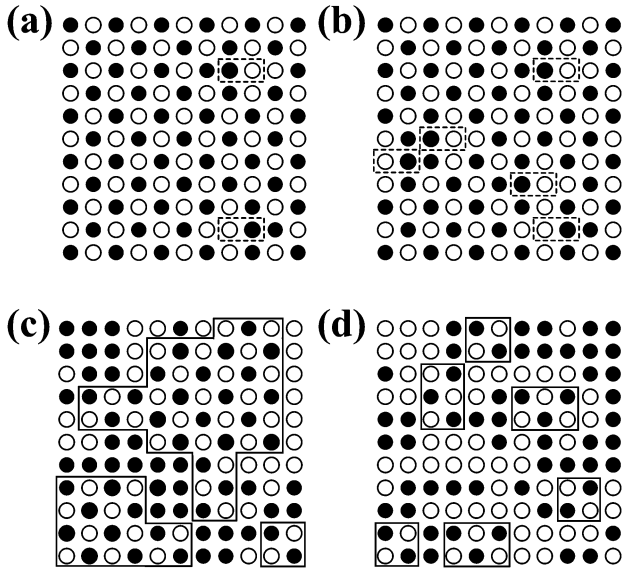

Figure 12. Expected Mn/Co atomic configuration: open circles, Mn; solid circles, Co. (a) Slowly cooled sample; $\langle S^a \rangle \approx 1$, $\langle s^a \rangle \approx 1$, δs^a = small. (b) 1373 K annealed sample; $\langle S^a \rangle \neq 0$, $\langle s^a \rangle \neq 0$, δs^a = relatively large. (c) 1423 K annealed sample; $\langle S^a \rangle = 0$, $\langle s^a \rangle \neq 0$, δs^a = large. (d) Quenched sample; $\langle S^a \rangle = 0$, $\langle s^a \rangle \neq 0$, δs^a = small. Dashed squares in (a) and (b) indicate Mn/Co ions at irregular site and solid squares in (c) and (d) indicate short-range Mn/Co atomic ordered regions.

range ordered ferromagnet. However, the samples showed a frequency dependence of χ' around T_C^m and magnetization relaxation at 5 K, which are often observed in a disordered system. Because the samples showed characteristics of long-range ordered ferromagnets, the disorder would originate from point defects such as Mn or Co ions at irregular site [squares in Figure 12a and b] or vacancies at the Mn/Co site due to the excess oxygen composition. Considering that the excess oxygen composition does not depend on T_a,[2] the T_a dependence of magnetic and calorimetric properties below T_C^a should be connected with a number of Mn or Co ions at an irregular site. The coercive force and retardation increased with increasing T_a up to T_C^a. This is understood by considering that a pinning force of a domain wall strengthens with increasing number of Mn or Co ions at an irregular site. The frequency-dependence parameter increased with increasing T_a. This is understood by considering that a large number of Mn or Co ions at an irregular site increases the distribution of pinning forces; namely, there are regions with a large amount of irregular atoms and with a small amount of irregular atoms. Such a distribution would increase the frequency-dependence parameter.

The samples quenched from above T_C^a showed the upward convex $\chi'^{-1}-T$ curve just above T_C^m, another anomaly in the $\chi'-T$ curve below T_C^m, asymmetric $M-H$ loop after high-field cooling, and unclear heat capacity anomaly around T_C^m. Because these were not observed in the samples annealed below T_C^a, these are connected with an absence of long-range Mn/Co atomic order. The upward convex $\chi'^{-1}-T$ curve just above T_C^m implies a formation of ferromagnetic clusters in a paramagnetic matrix because the inverse of $\chi = (1 - x)C_{para}/T + xC_{ferro}/(T - T_C)$ shows such a curvature just above T_C, where x is a fraction of the ferromagnetic component. Considering the presence of fluctuation of Mn/Co atomic order as shown in Figure 1, it is supposed that there exist Mn/Co atomic ordered regions (clusters) and disordered regions [see Figure 12c and d] in the samples quenched from above T_C^a and that the ferromagnetic clusters form within the short-range Mn/Co atomic ordered clusters. In fact, such a texture has been observed in the Ni_3Mn ferromagnetic arroy with partial order of Cu_3Au type.[13] The fluctuation of Mn/Co atomic order becomes large as T_C^a is approached, as indicated by Figure 1, which indicates that the sample becomes inhomogeneous as T_C^a is approached. This would be a reason for the result that the frequency-dependence parameter increases as T_a approaches T_C^a. The coercive force and retardation parameter also increased as T_a approaches T_C^a. This might be explained as follows. The ferromagnetic clusters in these samples would be a single ferromagnetic domain cluster because of the small size of the Mn/Co atomic ordered cluster. In this case, reversal of total magnetization occurs by rotation of magnetization in each ferromagnetic cluster (not displacement of domain walls). The rotation is difficult when the size of a single ferromagnetic domain cluster is large. Therefore, the reversal of total magnetization would become difficult and thus the coercive force and the retardation would increase as T_a approaches T_C^a.

Conclusions

$LaMn_{0.5}Co_{0.5}O_{3+\delta}$ samples whose Mn/Co atomic order was controlled were prepared by annealing at certain temperatures with successive quenching. It was found that the magnetic and calorimetric properties of $LaMn_{0.5}Co_{0.5}O_{3+\delta}$ qualitatively depend on whether the annealing temperature is above or below 1400 K, which suggests that an order−disorder phase transition with respect to the Mn/Co atomic configuration occurs at $T_C^a \approx 1400$ K. It is found that magnetic properties are classified into three groups correlated with the long-range order parameter, short-range order parameter, and order fluctuation with respect to the Mn/Co atomic configuration. The upward convex character in the $\chi'-T$ curve just above T_C^m, extra anomaly in the $\chi'-T$ curve below T_C^m, and asymmetric $M-H$ loop after high-field cooling seems to be observed only in the samples without the long-range order of the Mn/Co atomic configuration. T_C^m and magnetization under a high field are correlated with the short-range order parameter of the Mn/Co atomic configuration. A coercive force, magnetization retardation, and frequency dependence of the $\chi'-T$ peak intensity are correlated with the fluctuation of Mn/Co atomic order. The present results clearly indicate that fluctuation (inhomogeneity) and disorder with respect to atomic configuration should be distinguished to understand macroscopic magnetic properties.

Acknowledgment. Part of this work was financially supported by a Grant-in-Aid for Scientific Research from the Ministry of Education, Science, Culture, and Sports of Japan.

CM030279T

(13) Taoka, T. *J. Phys. Soc. Jpn.* **1956**, *11*, 537.